

# A statistical method for revealing form-function relations in biological networks

Andrew Mugler\*,<sup>1</sup> Boris Grinshpun,<sup>2,†</sup> Riley Franks,<sup>3</sup> and Chris H. Wiggins<sup>4</sup>

<sup>1</sup>*Department of Physics, Columbia University, New York, NY 10027*

<sup>2</sup>*Department of Applied Physics and Applied Mathematics, Columbia University, New York, NY 10027*

<sup>3</sup>*Department of Applied and Computational Mathematics,  
California Institute of Technology, Pasadena, CA 91125*

<sup>4</sup>*Department of Applied Physics and Applied Mathematics,  
Center for Computational Biology and Bioinformatics, Columbia University, New York, NY 10027*

Over the past decade, a number of researchers in systems biology have sought to relate the function of biological systems to their network-level descriptions — lists of the most important players and the pairwise interactions between them. Both for large networks (in which statistical analysis is often framed in terms of the abundance of repeated small subgraphs) and for small networks which can be analyzed in greater detail (or even synthesized in vivo and subjected to experiment), revealing the relationship between the topology of small subgraphs and their biological function has been a central goal. We here seek to pose this revelation as a statistical task, illustrated using a particular setup which has been constructed experimentally and for which parameterized models of transcriptional regulation have been studied extensively. The question “how does function follow form” is here mathematized by identifying which topological attributes correlate with the diverse possible information-processing tasks which a transcriptional regulatory network can realize. The resulting method reveals one form-function relationship which had earlier been predicted based on analytic results, and reveals a second for which we can provide an analytic interpretation. Resulting source code is distributed via <http://formfunction.sourceforge.net>.

The observation that form constrains function in biological systems has historical roots far older than systems biology. Century-old examples include those made in D’Arcy Thompson’s “On Growth and Form” [1] and the observation that the quick responses necessary for reflex actions such as heat- and pain-avoidance could be manifest only by a dedicated input-output relay circuit from fingers to brain and back [2]. Advances in synthetic biology, often requiring design of systems for which only topology can be specified without control over precise parameter values, has motivated a reintroduction of such topological thinking in biological systems [3–5]. A second source of such inquiry is high-throughput systems biology, in which technological advances provide topologies of large biological networks without precise knowledge of their interactions, dynamics, or possible naturally-occurring inputs [6–8]. Such limitations thwart our desire to learn form-function relations from data or to derive them from plausible first-principles modeling. Our goal here is to illustrate how re-framing the question as one of computation and statistical analysis allows a clear, quantitative, interpretable approach.

## I. SETUP

Mathematical progress requires clear definitions of terms, including, here, “form,” “function,” and “follow.”

To define the first two we must choose a specific experimental setup; we here choose one which has been experimentally realized repeatedly: that of a small, synthetic transcriptional regulatory network with “inducible promoters,” meaning that the efficacy of the transcription factors may be diminished by introducing small interfering molecules [5, 9–11] (Figure 1A). A common “output” responding to the “input” presence of such small molecules is the abundance of inducible green fluorescent protein (GFP), which provides an optical readout of one of the regulated genes. The “form,” then, will be defined by the topology of such a small regulatory network, distinguishing between up- and down-regulatory edges in the network.<sup>1</sup> “Function” will be defined by the realizable input-output relations of a device with two binary inputs (corresponding to presence or absence of the small molecules) and one real-valued output (the transcriptional level of the output gene).

Among other published experiments which correspond to this setup is that of Guet, et al. [9]. We remind the reader of two particularly noteworthy observations of Guet and coworkers: (i) that many of their experimentally-realized small networks were “broken” in the sense that the output remained constant over the different possible inputs; and (ii) that often the same topology can realize different input-output relations (or even be broken, i.e., can realize both a particular function as well as a lack of function entirely). Within a mathemat-

---

\*Current address: FOM Institute for Atomic and Molecular Physics (AMOLF), Science Park 104, 1098 XG Amsterdam; [mugler@amolf.nl](mailto:mugler@amolf.nl)

<sup>†</sup>[bg2178@columbia.edu](mailto:bg2178@columbia.edu)

---

<sup>1</sup> We use  $\rightarrow$  to indicate up-regulation,  $\dashv$  to indicate down-regulation, and  $\rightarrow$  to indicate regulation whose sign is not specified; additionally we use  $\rightsquigarrow$  to indicate inhibition by a small molecule.

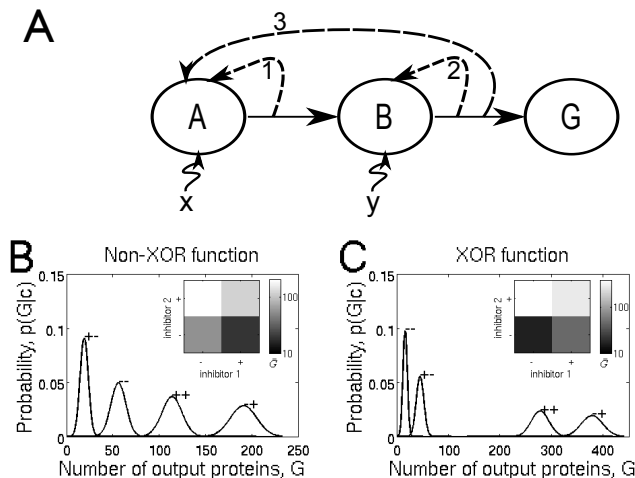


FIG. 1: Network set and input-output functions. (A) Transcription factor  $A$  regulates the expression of transcription factor  $B$ , which regulates the expression of fluorescent protein  $G$ . The efficacies of  $A$  and  $B$  are reduced by the presence of chemical inhibitors, labeled by scaling factors  $x$  and  $y$  (Eqn. 1), respectively. We distinguish between up- and down-regulation and consider all ways in which regulatory edges 1, 2, and 3 may appear, for a total of 160 networks. (B-C) Examples of non-XOR (B) and XOR (C) functions (see Sec. III A), as defined by the ranking of conditional probability distributions  $p(G|c)$ , where  $c \in \{-, -, -, +, +, +\}$  describes whether each inhibitor is present (+) or absent (-). Insets show mean protein number  $\bar{G}$  in each of the four states. The functions in B and C are both realized by the particular network in A in which edge 3 is absent and all remaining edges are down-regulating.

ical model, such behavior follows straightforwardly from considering the behavior of a given dynamical system at different points in the space of quantitative parameters [12]. Revealing such degeneracy of functions by exploring the parameter space given a topology (and given an algebraic expression modeling the regulatory interactions among the genes) may be recast as one of optimizing — locally in parameter space — the mutual information between input and output over this space [13–15]. Mutual information (MI) as a cost function is advantageous both biologically (in that many natural systems including transcriptional regulatory networks are known to operate near their information-optimal constraints [16–18]) and mathematically (in that by optimizing MI we can identify parameter settings which are functional without demanding in advance the particular input-output functions we seek). That is, we optimize for functionality rather than for a specific predetermined function.

MI between input and output is defined as a functional of the joint distribution  $p(c, G)$  — the probability of a (here, categorically-valued) setting of the chemistry and the (here, real-valued) concentration of the output gene (see Sec. II). The stochastic relationship between input in output in biological networks has many under-

lying sources; however, one source is intrinsic: the finite copy number of the constituent proteins introduces a “shot noise,” much discussed in the systems biology literature [19–23]. Particular additional sources of noise may thwart information processing as well in specific systems; hoping to remain as general as possible, we will here consider only intrinsic noise. In this respect, we aim to describe the functional response(s) of single cells, as opposed to an averaged response of a pooled population of cells.

Having defined form and function, we must define “follow.” Here we will need a measure of, for any topological feature of the networks, the extent to which the value of the feature (e.g., length of a cycle, number of down-regulations, etc.) does or does not correlate with the input-output relations the network can perform. Since we wish to correlate two categorical (rather than real-valued) features, MI is again useful, in that we will rank topological features by the information between its value and the particular input-output relations networks with that feature are found to perform.

To summarize: “function” is given by the possible input-output relations of which a given topology is capable; these are found by numerical optimization over parameters of the MI between input and output, with the probabilistic description of the transcriptional output set by intrinsic noise; “form” is mathematized by enumerating a list of topological attributes descriptive of our small networks. The question “how does function follow form” is here recast as a ranking of topological features based on the correlation (here, given by MI) between topological feature value and the particular input-output relations realizable for a given topology.

## II. METHOD

The method is illustrated in Fig. 2, which makes clear how the (general) search for form-function relations may be composed into separate tasks, the implementation of which is particular to one particular experimental setup. For example, the particular elements of the network set  $\Omega_n$  follow from system-specific choices made below, but the design of the task (Fig. 2) can be applied to relating form and function more generally. For a different experimental context, one or more of the “modules” in the design of the algorithm may need to be replaced, but the design itself we anticipate will be useful to revealing form-function relations in a wide variety of contexts.

Below we describe the method in detail as applied to our particular experimental setup; further information on networks, gene regulation, linear noise analysis, information theory, and optimization is provided in Sec. V.

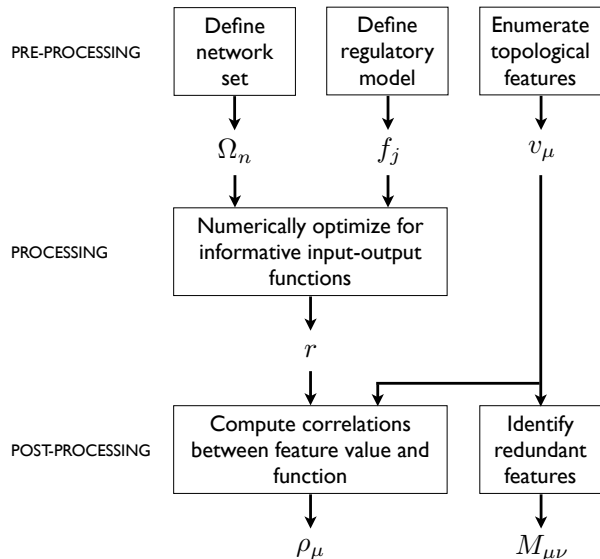


FIG. 2: Outline of the procedure used to ask “how does function follow form.” Variables are defined in text.

### A. Networks and features

We consider the simplest set of networks with two chemical inputs and one genetic output (Fig. 1A). Each of two chemical inhibitors is either present or absent, giving four possible input states. When present, the chemicals respectively inhibit two transcription factors, the second of which regulates the fluorescent output. We consider all ways in which each of the transcription factors may regulate itself and the other (with the constraint that neither is unregulated) and distinguish between up- and down-regulation, giving a total of 160 networks (the combinatorial accounting is presented in Sec. VA). The topology of each network  $n \in \{1, 2, \dots, 160\}$  constrains the model parameters  $\vartheta$  to lie within the particular feasibility set  $\Omega_n$ . Having defined the set of networks, we enumerate topological features and their values  $v_\mu$  (here,  $\mu \in \{1, 2, \dots, 17\}$ ; see Table I).

### B. Regulatory model

The mean protein numbers of the two transcription factors  $\bar{A}$  and  $\bar{B}$  and the fluorescent output  $\bar{G}$  are described by the deterministic dynamics

$$\begin{aligned} \frac{1}{R_A} \frac{d\bar{A}}{dt} &= \varphi_A(a, b) - \bar{A}, \\ \frac{1}{R_B} \frac{d\bar{B}}{dt} &= \varphi_B(a, b) - \bar{B}, \\ \frac{1}{R_G} \frac{d\bar{G}}{dt} &= \varphi_G(b) - \bar{G}, \end{aligned} \quad (1)$$

where  $a = \{\bar{A}/x, \bar{A}\}$  when the first inhibitor is {present, absent},  $b = \{\bar{B}/y, \bar{B}\}$  when the second inhibitor is {present, absent}, and the  $R_j$  are degradation rates ( $j \in \{A, B, G\}$ ). The parameters  $x > 1$  and  $y > 1$  model the effect of the interfering small molecules by reducing the effective concentrations of the proteins. This gives a total of four chemical input states denoted  $c \in \{-, -, +, +\}$ , each state describing whether each of the two inhibitors is present (+) or absent (-). The terms  $\varphi_j$  describe the transcriptional regulation of each species by its parent(s) and are formulated under a statistical mechanical model [24–26]. The statistical mechanical approach to modeling transcription is principled, compact, and in the case of combinatorial regulation [24] captures the diversity of multidimensional responses observed in experimental systems [27–29]. Full algebraic forms of the  $\varphi_j$  are dependent on topology, including, in the case of combinatorial regulation, whether the transcription factor interaction is additive or multiplicative (see Sec. VB1).

The stochastic description of each network is set by intrinsic noise. We obtain probability distributions over protein numbers using the linear noise approximation (LNA) [20, 30, 31], since, in contrast to simulation techniques [19], the LNA does not rely on sampling and is thus much more computationally efficient (making many-parameter optimization feasible). Under the LNA the steady state distribution over each species’ protein number is a Gaussian expansion around the deterministic mean given by the steady state of Eqn. 1. The covariance matrix  $\Xi$  under the LNA is determined from model parameters by (numerically) solving the Lyapunov equation  $J\Xi + \Xi J^T + D = 0$ , where  $J$  is the Jacobian of the system in Eqn. 1 and  $D = \text{diag}\{R_A(\varphi_A + \bar{A}), R_B(\varphi_B + \bar{B}), R_G(\varphi_G + \bar{G})\}$  is an effective diffusion matrix. Of particular importance are the distributions  $p(G|c)$ , the stochastic response of the output species  $G$  given that the system is in each of the four input states  $c$ . The input-output MI may be computed directly from this quantity,  $I[p(c, G)] = \sum_c \int dG p(G|c) p(c) \log[p(G|c) / \sum_{c'} p(G|c') p(c')]$ , with the provision that the input states are equally likely,  $p(c) = 1/4$ .

### C. Input-output functions

The possible input-output responses of each network are found by locally optimizing MI in parameter space. The optimization is done numerically using MATLAB’s `fminsearch` and initialized by sampling uniform-randomly in the logs of the parameters (specific bounds from which initial parameters are sampled are given in Table II). The optimization is performed at constrained average protein number  $N \equiv (\bar{A} + \bar{B} + \bar{G})/3$  and average timescale separation  $T \equiv [(R_A + R_B)/2]/R_G$  by maximizing the quantity  $L \equiv I - \eta N - \kappa T$  for various values of the Lagrange multipliers  $\eta$  and  $\kappa$  ( $R_G$  is fixed).

Optimization of MI has the effect of increasing the separation among the distributions  $p(G|c)$  (see Fig. 1B-C). To reflect the fact that many observed regulatory networks are known to operate near their information-optimal limits [16–18], we use in the statistical analysis only those optimal solutions whose MI lies above a cutoff value. Choosing a cutoff larger than 1.5 bits (which corresponds to two fully separated distributions and two fully overlapping distributions) ensures that the means of the distributions are fully resolved, and thus allows one to define the function performed by the network as the ranking  $r$  of the means of the distributions  $p(G|c)$  along the  $G$  axis. For the results in this study we use a cutoff of 1.55 bits. The method can be easily extended to include less informative locally optimal functions, e.g. binary logic gates such as an AND function, by using a lower MI cutoff and generalizing the definition of function as ranking [14]. Fig. 1B-C shows examples of two different functions performed by the same network that are local optima in MI at different points in parameter space; they correspond to  $r = 1$  and  $r = 9$  on the horizontal axis of Fig. 5, respectively.

To correct for repeated sampling of the same local optimum at close but numerically distinct points in the real-valued parameter space, nearest-neighbor optima performing the same function are merged. This enforces that the distribution of optimal parameters is sampled uniformly. The robustness of subsequent results to this choice is tested numerically (see Sec. III B).

#### D. Correlating feature value and function

For each topological feature  $\mu$ , the correlation between feature value  $v_\mu$  and function  $r$  is computed from the joint probability distribution  $p(v_\mu, r)$ . This distribution is defined by the optimization data and the factorization

$$\begin{aligned} p(v_\mu, r) &= \sum_{\vartheta, n} p(v_\mu, r, \vartheta, n) = \sum_{\vartheta, n} p(v_\mu, r | \vartheta, n) p(\vartheta, n) \\ &= \sum_{\vartheta, n} p(v_\mu | n) p(r | \vartheta, n) p(\vartheta | n) p(n), \end{aligned} \quad (2)$$

where  $\vartheta$  runs over all points in parameter space at which an optimum is found. Here  $p(v_\mu | n)$  is  $\{0, 1\}$ -valued, set by whether network  $n$  has value  $v$  for feature  $\mu$ ; and  $p(r | n, \vartheta)$  is  $\{0, 1\}$ -valued, set by whether network  $n$  performs function  $r$  at point  $\vartheta$ , according to the optimization data. The distributions  $p(\vartheta | n)$  and  $p(n)$  are assumed to be “flat,” i.e.  $p(\vartheta | n) = 1/|\vartheta|_n$  and  $p(n) = 1/|n|$ , where  $|\vartheta|_n$  is the number of distinct local optima in parameter space for network  $n$ , and  $|n|$  is the number of networks; the robustness of subsequent results to weakening either of these assumptions is tested numerically (see Sec. III B).

The correlation between feature value and function is computed as their MI, normalized by the entropy of

$p(v_\mu)$ , to yield a statistic

$$\rho_\mu \equiv \frac{I[p(v_\mu, r)]}{H[p(v_\mu)]} \quad (3)$$

that ranges from 0 (when the function provides no information about the feature value) to 1 (when the feature value is exactly determined by the function).

### III. RESULTS

#### A. Non-parametric analysis

We first present an analysis which requires no assumptions about what is a “flat” distribution in parameter space, i.e., we simply enumerate how many networks are capable of a given degeneracy of input-output functions, and how many input-output functions may be realized by a given multiplicity of networks (Fig. 3). This analysis recovers an intuitive result (Fig. 3A): that “XOR” functions, in which the sign of the influence of one input depends on the value of the other, are more difficult to realize (i.e. they are observed in fewer networks). Simpler functions, in which the influence of one input remains positive or negative irrespective of the value of the other, are easier to realize. The analysis also reveals that each network can perform at least two functions (Fig. 3B). These are the two functions consistent with the signs of the forward regulatory edges  $A \rightarrow B$  and  $B \rightarrow G$ , as described in detail in Sec. III D. Since the topology  $A \rightarrow B \rightarrow G$  is that obtained in the parametric limit when the feedback edges are of negligible strength, it is clear that these functions must be realizable; Fig. 3B shows further that these functions are sufficiently informative to be observed as information-optima.

#### B. Topological features and robustness

Table I ranks the topological features by  $\rho$ , which measures how uniquely form determines function. Recall that in computing  $\rho$  from  $p(v_\mu, r)$  we assume that the distributions  $p(n)$  and  $p(\vartheta | n)$  are both uniform (Eqn. 2); we find that the ranking in Table I is robust to deviations of both distributions from uniformity, as demonstrated by the following numerical experiments.

The uniformity of  $p(n)$  is perturbed by artificially setting  $p(n) \propto (u_n)^\epsilon$ , where  $u_n$  is a vector of random numbers and  $\epsilon$  tunes the entropy of the distribution, i.e.  $\epsilon = 0$  recovers the maximum-entropy (uniform) distribution, while  $\epsilon \rightarrow \infty$  produces the zero-entropy distribution  $p(n) = 1 \Leftrightarrow n = \operatorname{argmax}(u_n)$ . We find that the ranking of the top 4 features is preserved under  $\sim 15\%$  perturbations in the entropy, and that the ranking of the top 3 features is preserved under  $\sim 30\%$  perturbations (see Fig. 7A). This demonstrates that the feature ranking is considerably robust to perturbations in the uniformity of  $p(n)$ .

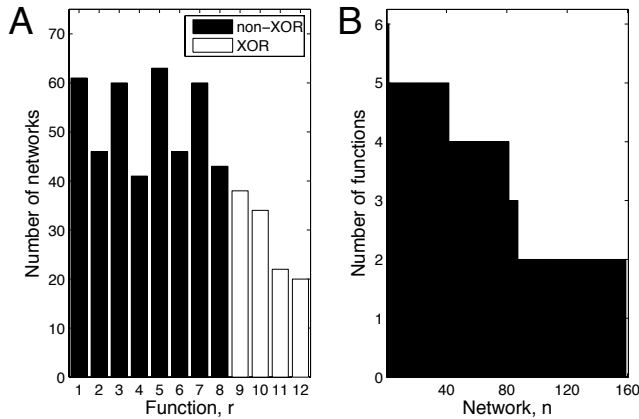


FIG. 3: Non-parametric analysis of network functionality. (A) Histogram showing how many networks can perform each input-output function. Functions are numbered along the horizontal axis as in Fig. 5. (B) Histogram showing how many input-output functions may be realized by each network. The order of networks along the horizontal axis is determined by ranking according to number of functions realized.

Topological feature	$\rho$
1. Sign of forward edges	0.92366
2. Number of up-regulating edges	0.18249
3. Number of down-regulating edges	0.18098
4. Sign of autoregulation of species $B$	0.03228
5. Number of positive feedback cycles	0.01133
6. Number of negative feedback cycles	0.01109
7. Nesting structure of feedback cycles	0.00418
8. Type of interaction of edges into $B$	0.00288
9. Number of edges	0.00184
10. Number of feedback cycles	0.00184
11. Sign of $A$ - $B$ feedback cycle	0.00173
12. Number of additive interactions	0.00141
13. Type of interaction of edges into $A$	0.00085
14. Number of nested feedback cycles	0.00081
15. Sign of autoregulation of species $A$	0.00058
16. Number of multiplicative interactions	0.00048
17. Sign of edge $B \rightarrow A$	0.00021

TABLE I: Topological features ranked by correlation measure  $\rho$ .

The uniformity of  $p(\vartheta|n)$  is perturbed similarly, and we find that the ranking of the top 7 features is preserved under  $\sim 40\%$  perturbations in the entropy of  $p(\vartheta)$  (see Fig. 7B). In this case we also have an independent entropy scale, given by the fact that we may decompose  $p(\vartheta|n)$  as  $p(\vartheta|n) = \sum_{\vartheta_0} p(\vartheta|\vartheta_0, n)p(\vartheta_0|n)$ , where  $\vartheta_0$  is the parameter setting that initializes an optimization and  $p(\vartheta|\vartheta_0, n)$  is determined by the optimization itself. If we assume uniformity of  $p(\vartheta_0|n)$ , instead of  $p(\vartheta|n)$ , then  $p(\vartheta|n)$  is computable from the numbers of times the op-

timization converges repeatedly on each local optimum  $\vartheta$ . The entropy in this case is 13% different from that of the uniform distribution, and the ranking of  $\rho$  is almost entirely unchanged (Fig. 7B). This observation demonstrates that the results are not sensitive to whether one takes the distribution of initial parameters or the distribution of optimal parameters to be uniform.

### C. Non-redundant features

Many topological features are not independent; for example, the feature “number of up-regulating edges” is highly correlated with “number of down-regulating edges.” To interpret which features are associated with which sets of realizable functions, it is useful to group nearly identical features together and use only the feature which is most informative about function (highest in  $\rho$ ) as the exemplar among each group. To quantify redundancy among features, we compute the MI between each pair of features and normalize by the minimum entropy to produce a weighted adjacency matrix  $M_{\mu\nu} = I[p(v_\mu, v_\nu)] / \min\{H[p(v_\mu)], H[p(v_\nu)]\}$ , which we then use as the basis for unidimensional scaling [32] (see Sec. VF).

Fig. 4 plots features’  $\rho$  values against the unidimensional scaling coordinate, revealing two distinct groups of highly informative features. The first, which includes the features ranked 1, 2, 3, 5, and 6, is dominated by feature 1: the signs (up- or down-regulating) of the forward regulatory edges  $A \rightarrow B$  and  $B \rightarrow G$ . The second, which includes the features ranked 4, 8, 11, and 12, is dominated by feature 4: the sign (up-regulating, down-regulating, or absent) of the autoregulation of species  $B$ . The high information content of each of these two features is revealed visually by inspection of the conditional distribution  $p(r|v_\mu) = p(v_\mu, r)/p(v_\mu)$  (Fig. 5), as described in detail in the next sections. The functional importance of both of these features is supported by analytic results; for the first feature these analytic predictions were made in earlier work [14] and are recalled here, while for the second feature new analytic results are derived here.

### D. Forward regulation

The topological feature that is most informative of network function is feature 1: the signs of the forward regulatory edges  $A \rightarrow B$  and  $B \rightarrow G$ . Inspection of the feature value–function conditional distribution  $p(r|v)$  in Fig. 5A reveals a rich, highly organized (and thus highly informative) structure which we here interpret.

The most prominent aspect of the probability matrix in Fig. 5A is the high-probability double-diagonal spanning the eight non-XOR functions (i.e. functions 1 and 2 are most often performed by networks with the first feature value, functions 3 and 4 the second feature value, functions 5 and 6 the third feature value, and functions 7

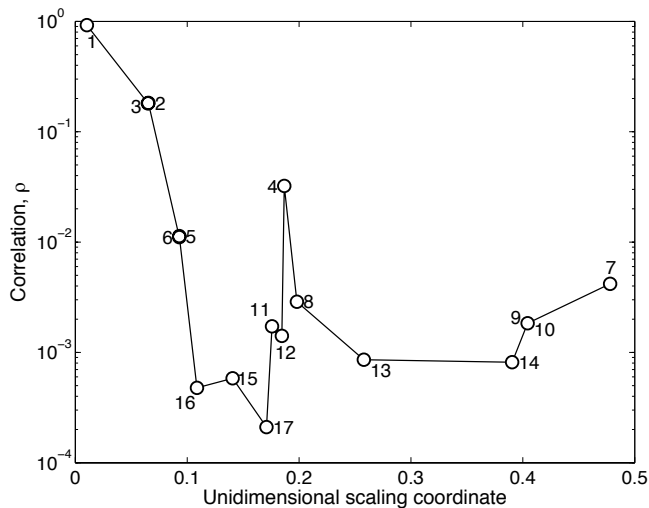


FIG. 4: Identifying feature redundancy. Correlation measure  $\rho$  is plotted against a unidimensional scaling coordinate which groups similar features together (i.e. the components of the eigenvector corresponding to the largest-magnitude eigenvalue of the feature adjacency matrix  $M_{\mu\nu}$ ). Features are numbered by rank (Table I).

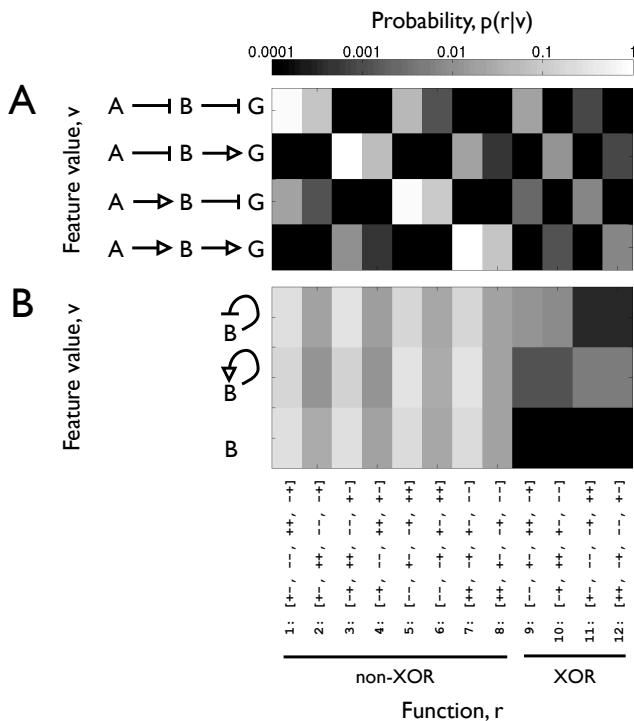


FIG. 5: Conditional distributions showing the probability of a particular input-output function given the value of a topological feature, for two features: (A) the signs (up- or down-regulating) of the forward regulations, and (B) the sign (up-regulating, down-regulating, or absent) of the autoregulation of species  $B$ .

and 8 the fourth feature value). These are the functions one would expect by looking at the forward edges alone, i.e. in the absence of feedback. For example, in networks with the last feature value,  $A \rightarrow B \rightarrow G$ , inhibition of  $A$  and of  $B$  will both reduce the expression of  $G$ , such that the state in which both small molecules are present ( $++$ ) produces the lowest-ranked output, and conversely, the state in which both small molecules are absent ( $--$ ) produces the highest-ranked output; functions 7 and 8 are the two that satisfy these criteria. In previous work [14] we termed these functions “direct,” and we showed analytically that networks are limited to direct functions even when feedback is added, so long as each species is regulated by at most one other species. This fact is validated here numerically: a plot of  $p(v|r)$  for only those networks in our set in which each species is regulated by one other species shows nonzero entries only for the direct functions (Fig. 9).

Among all networks, including those with combinatorial feedback (i.e. two edges impinging on one node), we see that direct functions still dominate, indicated by the bright double-diagonal in Fig. 5A. Networks with combinatorial feedback perform other functions as well, but more rarely; examples include those functions in Fig. 5A above and below the double-diagonal and XOR functions 9-12. The performance of these additional functions remains well organized by feature value, which makes the signs of the forward edges a highly informative feature.

### E. Autoregulation of $B$

Other than feature 1 (and the features highly correlated with feature 1), the most informative feature is feature 4: the autoregulation of species  $B$ . Inspection of its feature value–function distribution (Fig. 5B) reveals that the information content lies in the ability to perform XOR functions. Specifically, networks in which  $B$  is autoregulated are observed to perform XOR functions, while networks in which  $B$  is not autoregulated are not observed to perform XOR functions. Indeed, autoregulation has been observed to enhance the functional response to multiple inputs in a related study in the context of Boolean logic gates [33].

XOR functions are those in which the sign of the influence of one input depends on the value of the other; mathematically they satisfy one or both of two properties:

XOR property I:  $\text{sign}(d\bar{G}/dx)$  depends on  $y$ ,

XOR property II:  $\text{sign}(d\bar{G}/dy)$  depends on  $x$ ,

The four observed XOR functions satisfy property I (e.g. Fig. 1C inset); no functions satisfying property II are observed (Fig. 5B). Analytic support for these facts is obtained by calculating  $d\bar{G}/dx$  and  $d\bar{G}/dy$ , respectively.

To understand why autoregulation of  $B$  is necessary for XOR functions satisfying property I, we calculate  $d\bar{G}/dx$

analytically. We obtain (see Sec. V H 1)

$$\frac{d\bar{G}}{dx} = \frac{1}{-\Delta} \frac{\partial a}{\partial x} \frac{\partial \varphi_B}{\partial a} \frac{\partial \varphi_G}{\partial \bar{B}}, \quad (4)$$

where  $\Delta = (\partial \varphi_A / \partial \bar{B})(\partial \varphi_B / \partial \bar{A}) - [(\partial \varphi_A / \partial \bar{A}) - 1][(\partial \varphi_B / \partial \bar{B}) - 1]$  is the determinant of the Jacobian of the dynamical system in Eqn. 1 and is always negative for stable fixed points. Eqn. 4 has an intuitive form when considering the direct path from  $x$  to  $G$  (Fig. 1A): the term  $\partial a / \partial x = -\bar{A} / x^2 < 0$  corresponds to the inhibitory signal  $x \rightsquigarrow A$ , the term  $\partial \varphi_B / \partial a$  corresponds to the regulatory edge  $A \rightarrow B$ , and the term  $\partial \varphi_G / \partial \bar{B}$  corresponds to the regulatory edge  $B \rightarrow G$ . Since  $G$  has only one regulatory input,  $\varphi_G(b)$  is monotonic, making  $\partial \varphi_G / \partial \bar{B} = (d\varphi_G / db)(\partial b / \partial \bar{B}) = (d\varphi_G / db) / y$  of unique sign. The same is true for  $\partial \varphi_B / \partial a$  when  $B$  has only one regulatory input (i.e. when  $B$  is not autoregulated). However when  $B$  has more than one regulatory input (i.e. when  $B$  is autoregulated), the sign of  $\partial \varphi_B / \partial a$  can depend on  $y$ , allowing XOR property I. Specifically, under our regulatory model, when  $B$  is autoregulated,  $\partial \varphi_B / \partial a$  is the product of a positive term and a term quadratic in  $b = \bar{B} / y$  that has positive roots for some parameter settings (see Sec. V H 2). This analysis suggests inspection of the parameters themselves obtained via optimization; doing so, we observe that the vast majority of observed XOR functions result from optimal parameter values for which there exists a positive root in the range  $0 < \bar{B} / y < \sim 100$ , which is the range of protein numbers in which our optimal solutions lie (Fig. 1B-C). To summarize, non-monotonicity in the regulation of species  $B$ , which can occur only when  $B$  is autoregulated, produces the observed XOR functions.

To understand why XOR functions satisfying property II are not observed, we calculate  $d\bar{G} / dy$  analytically. We obtain (see Sec. V H 1)

$$\frac{d\bar{G}}{dy} = \frac{1}{-\Delta} \left( 1 - \frac{\partial \varphi_A}{\partial \bar{A}} \right) \frac{\partial b}{\partial y} \frac{d\varphi_G}{db}, \quad (5)$$

where as before the determinant  $\Delta$  is always negative. The last two terms correspond to edges along the direct path from  $y$  to  $G$ , i.e.  $y \rightsquigarrow B$  and  $B \rightarrow G$  respectively, and are of unique sign; the term in parentheses describes the effect of the upstream species  $A$  and feedback. In all optimal solutions the term in parentheses is observed to be positive, despite wide variations in the orders of magnitude of each of the optimal parameters across solutions. This observation is largely explained by a stability analysis: for four of the six possible topological classes of networks (those in which  $A$  is singly, not doubly, regulated; Fig. 1A), stability of a fixed point of Eqn. 1 implies that the term in parentheses is positive; for the other two topological classes, stability implies that this term is greater than a quantity that is zero for some parameter settings and of unknown sign for others (see Sec. V H 3). In this last case it is unclear whether negative values of this term are analytically forbidden or simply exceedingly

unlikely given the regulatory model and the space of optimal solutions. Empirically this term is always positive, and type-II XOR functions are not observed.

The necessity of both forward regulation and autoregulation of species  $B$  for the performance of XOR functions highlights the importance of combinatorial regulation in functional versatility. As previously mentioned, networks without combinatorial regulation are limited to a particular class of functions which does not include XOR functions [14]. Moreover, in the original experiment of Guet et al. [9], each species was singly regulated, and accordingly no XOR functions were observed.

## IV. DISCUSSION

Both in order to assign functional significance to observed small network topologies in nature, and to design synthetic networks which will execute a desired function or set of functions, it is useful to develop a systematic approach for revealing the extent to which the form of a small network guides or constrains its functions. Resorting to hypothesized functions may be appealing in terms of interpretability, but this strategy risks overemphasizing those functions which one is looking for, or overlooking an unexpected function entirely.

The statistical analysis, along with the analytic results presented above, illustrate how the search for form-function relations can be posed as an algorithmic approach leading to interpretable mechanisms. While we have illustrated it for a particular, experimentally-realized setup, the approach itself, subdivided into a set of distinct modules in Fig. 2, we anticipate will be applicable to a wide variety of biophysical contexts. Similarly, we have chosen a framework from which much can be discovered by analytic study of the deterministic dynamical system; other experimental setups may require vastly different analytic explanations, but the idea of using statistical methods to highlight the features of paramount importance should be implementable as illustrated. We look forward to exploring the extent to which form does or does not follow function — and how — in related biophysical and biochemical models of small information processing networks in biology.

## V. APPENDIX

The remainder of this paper contains details on the set of networks studied, the regulatory model, the optimization procedure, and the statistical analysis used to identify exemplars among non-redundant groups of topological features. Additionally, it includes further background on information theory and the linear noise approximation. Finally, it presents numerical and analytic results as referenced in the main text, including numerical tests of the robustness of results to uniformity assumptions made in the statistical analysis, statistical validation of

an analytically derived functional constraint, and analytic results on the ability of networks to perform XOR functions.

### A. Networks

Many researchers over the past decades have begun to focus on the description of a given biological system not in terms of the isolated functions of its independent components, but in terms of the collective function of the network of interacting components as a whole. A central example of such a network is that describing interactions among genes: many genes produce proteins called transcription factors, whose role is to influence the protein production of other genes. The goal of the present study is, for a set of such networks, to develop a statistical method for determining the extent to which the topology of the network correlates with the function(s) it performs. In this section we describe the set of networks considered, including presentation of its combinatorics.

We consider the set of networks consisting of two transcription factors  $A$  and  $B$ , each of which can be chemically inhibited, each of which is regulated by itself, the other, or both, and one of which regulates the expression of a fluorescent output gene  $G$  (Fig. 1A). We distinguish between up- and down-regulating edges, and, in the case of more than one regulatory input edge, between additive and multiplicative interaction of the transcription factors (see model in next section). This gives a set of 160 networks, as described by the combinatorics here.

There are six ways in which the three possible feedback edges illustrated in Fig. 1A can appear such that species  $A$  remains regulated. In 2 configurations (Figs. 6A-B), both  $A$  and  $B$  are singly regulated, and there are a total of 3 edges per configuration, each of which can be up- or down-regulating. The number of networks is thus  $[\text{number of configurations}] \times [2^{\text{(number of edges)}}] = [2] \times [2^{(3)}] = 16$ .

In 3 configurations, (Fig. 6C-E), one of  $A$  and  $B$  is singly regulated while the other is doubly regulated. In the case of double regulation, the interaction between transcription factors is either (i) additive, in which the signs (up or down) of the two regulatory edges are independent, giving 4 possibilities, or (ii) multiplicative, in which the two regulatory edges have the same sign, giving 2 possibilities (see model in next section), for a total of 6 possibilities. The number of networks is thus  $[\text{number of configurations}] \times [2^{\text{(number of singly regulated nodes)}}] \times [6^{\text{(number of doubly regulated nodes)}}] = [3] \times [2^{(2)}] \times [6^{(1)}] = 72$ .

In the last configuration (Fig. 6F), both  $A$  and  $B$  are doubly regulated, and the number of networks is  $[\text{number of configurations}] \times [2^{\text{(number of singly regulated nodes)}}] \times [6^{\text{(number of doubly regulated nodes)}}] = [1] \times [2^{(1)}] \times [6^{(2)}] = 72$ . This gives a total of  $16 + 72 + 72 = 160$  networks.

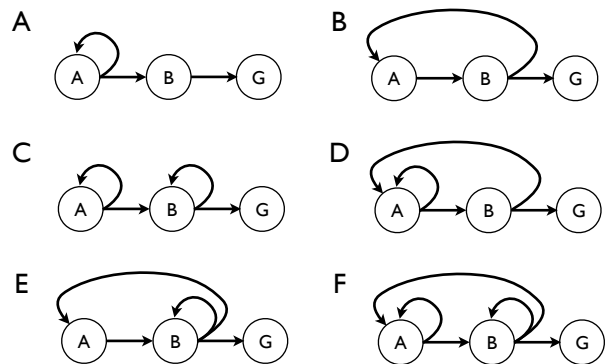


FIG. 6: The six possible topological configurations of the networks studied.

### B. Gene regulation

A regulatory network is most simply described using a dynamical system whose degrees of freedom are the concentrations of its constituent proteins. The nature of the interactions is then determined by the functional form of regulatory production terms on the righthand side of the dynamical system. In this study we formulate production terms under a statistical mechanical model [24–26] that has been shown to capture diverse functionality in the case of combinatorial regulation [24].

Because many proteins are present in cells in as few as tens or hundreds of copies [34], a deterministic dynamical system, which ignores intrinsic fluctuations around mean protein concentrations, can provide an insufficient description of the biological system when copy numbers are low. Ideally one instead seeks to solve the *master equation*, which describes the dynamics of the *probability* of observing given protein numbers. Unfortunately, almost all master equations describing regulatory networks, including the set of small networks we study here, are intractable analytically. As a result, several techniques to simulate [19] or approximate [31] the master equation have been developed; we here employ the *linear noise approximation* (LNA). Since the LNA does not rely on sampling (in contrast to simulation techniques), it is computationally efficient, which makes feasible the many-parameter optimization performed in this study.

The LNA is a second-order expansion of the master equation, with the first-order terms recovering the deterministic description. Therefore, in the present section, we first describe in detail the regulatory model used in the deterministic system; then we describe the LNA and its application to our networks.



### 1. Deterministic description: Dynamical system

As in Eqn. 1, the mean protein numbers of the three species are described by the following deterministic dynamics (for notational brevity the bars have been dropped — i.e. the quantities  $\bar{A}$ ,  $\bar{B}$ , and  $\bar{G}$  have been changed to  $A$ ,  $B$ , and  $G$  — and the regulation terms  $\varphi_A$ ,  $\varphi_B$ , and  $\varphi_G$  have been relabeled  $\alpha$ ,  $\beta$ , and  $\gamma$ , respectively):

$$\frac{1}{R_A} \frac{dA}{dt} = \alpha(a, b) - A, \quad (6)$$

$$\frac{1}{R_B} \frac{dB}{dt} = \beta(a, b) - B, \quad (7)$$

$$\frac{1}{R_G} \frac{dG}{dt} = \gamma(b) - G, \quad (8)$$

where  $a = \{A/x, A\}$  when the first inhibitor is {present, absent},  $b = \{B/y, B\}$  when the second inhibitor is {present, absent}, and the  $R_j$  are degradation rates ( $j \in \{A, B, G\}$ ). The parameters  $x > 1$  and  $y > 1$  incorporate the inhibition by reducing the effective concentrations of the proteins. This gives a total of four chemical input states  $c \in \{-, -, +, +\}$ , each state describing whether each of the two inhibitors is present (+) or absent (-).

*a. Stability* Steady state solutions of the dynamical system in Eqns. 6-8 are stable fixed points, i.e. points at which the all eigenvalues of the Jacobian have negative real part. The Jacobian of the system is

$$J = \begin{pmatrix} \frac{\partial \alpha}{\partial A} - 1 & \frac{\partial \alpha}{\partial B} & 0 \\ \frac{\partial \beta}{\partial A} & \frac{\partial \beta}{\partial B} - 1 & 0 \\ 0 & \frac{\partial \gamma}{\partial B} & -1 \end{pmatrix}. \quad (9)$$

Its eigenvalues are

$$\lambda_{1,2} = \frac{1}{2} \left[ \frac{\partial \alpha}{\partial A} + \frac{\partial \beta}{\partial B} - 2 \pm \sqrt{\left( \frac{\partial \alpha}{\partial A} - \frac{\partial \beta}{\partial B} \right)^2 + 4 \frac{\partial \alpha}{\partial B} \frac{\partial \beta}{\partial A}} \right] \quad (10)$$

and  $\lambda_3 = -1$ . At stable fixed points  $\text{Real}\{\lambda_{1,2}\} < 0$ ; equivalently the determinant of Eqn. 9, which is real and equal to the product of the eigenvalues, must be negative:

$$\begin{aligned} \Delta &\equiv \det(J) = \lambda_1 \lambda_2 \lambda_3 \\ &= \frac{\partial \alpha}{\partial B} \frac{\partial \beta}{\partial A} - \left( \frac{\partial \alpha}{\partial A} - 1 \right) \left( \frac{\partial \beta}{\partial B} - 1 \right) < 0. \end{aligned} \quad (11)$$

*b. Regulation terms* The regulatory model is that of Buchler et al. [24], in which the protein production is proportional to the probability that the RNA polymerase (RNAP) is bound to the promoter of interest. This probability is formulated thermodynamically, i.e. by enumerating and statistically weighting all ways in which transcription can and cannot occur.

For our networks, the regulation terms  $\alpha$ ,  $\beta$ , and  $\gamma$  are

$$\alpha(a, b) = \frac{s_A}{R_A} p_A(a, b), \quad (12)$$

$$\beta(a, b) = \frac{s_B}{R_B} p_B(a, b), \quad (13)$$

$$\gamma(b) = \frac{s_G}{R_G} p_G(b), \quad (14)$$

where the  $s_j$  are promoter strengths, and the probabilities of transcription  $p_j$  are given by

$$p_j = \frac{Z_{\text{on}}^j}{Z_{\text{on}}^j + Z_{\text{off}}^j}. \quad (15)$$

The partition functions  $Z_{\text{on}}^j$  and  $Z_{\text{off}}^j$  describe all the ways that transcription can occur and not occur, respectively, at the promoter region of gene  $j$ . As presented in detail below, the partition functions are determined by network topology and depend on additional parameters, including interaction strengths  $w$ , binding constants  $K$ , and “leakiness”  $q$  (i.e. the statistical weight given to bare binding of the RNAP). All parameters are positive. We first offer qualitative interpretation of the parameters, then we present the detailed expressions for the partition functions.

The  $w$  describe the interaction strengths between transcription factors, or between a transcription factor and the RNAP. Alphabetical superscripts refer to the promoter regions of genes  $A$ ,  $B$ , or  $G$ , while numerical subscripts refer to the molecules involved in the interaction: RNAP (0), transcription factor  $A$  (1), or transcription factor  $B$  (2). For example,  $w_{01}^B$  describes the interaction between RNAP and transcription factor  $A$  at the promoter region of gene  $B$ .

The signs of the logs of the  $w_{0i}^j$  determine the signs of the edges (where  $j \in \{A, B, G\}$  for the three promoter regions and  $i \in \{1, 2\}$  for transcription factors  $A$  and  $B$ ). For example,  $w_{01}^B$  describes the regulation of species  $B$  by species  $A$ ; if  $\log w_{01}^B > 0$  then the edge  $A \rightarrow B$  is up-regulating, and if  $\log w_{01}^B < 0$  then the edge  $A \rightarrow B$  is down-regulating.

Following the model of Buchler et al. [24], when two transcription factors regulate one species, they may do so “independently” or “synergistically.” Independent regulation corresponds to the case when both transcription factors interact with the same domain of the RNAP; mathematically the interaction strengths are additive ( $w_{01}^j + w_{02}^j$ ). If the RNAP has several interaction domains, two transcription factors can interact synergistically, and the interaction strengths are multiplicative ( $w_{01}^j w_{02}^j$ ). Synergistic regulation implies the additional constraint that the regulatory effects of the two transcription factors (i.e. the logs of the interaction strengths) are of the same sign.

The  $K$  describe the binding constants of each transcription factor to each promoter region. They have super- and subscripts similar to the  $w$ , e.g.  $K_1^B$  describes the binding of transcription factor  $A$  to the promoter region of gene  $B$ .

The partition functions  $Z_{\text{on/off}}^j$  for the network topologies shown in Fig. 6 are presented below. To provide intuition, the first two expressions are interpreted in detail.

Topology A is shown in Fig. 6A; its partition functions are

$$Z_{\text{on}}^A = q + w_{01}^A q \frac{a}{K_1^A}, \quad (16)$$

$$Z_{\text{off}}^A = 1 + \frac{a}{K_1^A}, \quad (17)$$

$$Z_{\text{on}}^B = q + w_{01}^B q \frac{a}{K_1^B}, \quad (18)$$

$$Z_{\text{off}}^B = 1 + \frac{a}{K_1^B}, \quad (19)$$

$$Z_{\text{on}}^G = q + w_{02}^G q \frac{b}{K_2^G}, \quad (20)$$

$$Z_{\text{off}}^G = 1 + \frac{b}{K_2^G}. \quad (21)$$

Eqn. 16 describes the two ways in which transcription can occur at the promoter region of gene  $A$ : (i) the RNAP can bind unassisted, with statistical weight  $q$ , or (ii) since  $A$  is self-regulating, the RNAP can bind upon interaction with transcription factor  $A$ , with weight proportional to  $q$  for the RNAP, to the effective concentration  $a$  scaled by the binding constant  $K_1^A$  for transcription factor  $A$ , and to the interaction strength  $w_{01}^A$  between the RNAP and transcription factor  $A$ . Eqn. 17 describes the two ways in which transcription can not occur at the promoter region of gene  $A$ : (i) there can be nothing bound, an outcome whose statistical weight we are free, via the normalization enforced in Eqn. 15, to set, and so we set to 1, and (ii) the transcription factor alone can bind, with weight  $a/K_1^A$ . Eqns. 18-21 are similarly derived according to the topology of the network.

Topology B is shown in Fig. 6B; its partition functions are

$$Z_{\text{on}}^A = q + w_{02}^A q \frac{b}{K_2^A}, \quad (22)$$

$$Z_{\text{off}}^A = 1 + \frac{b}{K_2^A}, \quad (23)$$

$$Z_{\text{on}}^B = q + w_{01}^B q \frac{a}{K_1^B}, \quad (24)$$

$$Z_{\text{off}}^B = 1 + \frac{a}{K_1^B}, \quad (25)$$

$$Z_{\text{on}}^G = q + w_{02}^G q \frac{b}{K_2^G}, \quad (26)$$

$$Z_{\text{off}}^G = 1 + \frac{b}{K_2^G}. \quad (27)$$

Topology C is shown in Fig. 6C; its partition functions

are

$$Z_{\text{on}}^A = q + w_{01}^A q \frac{a}{K_1^A}, \quad (28)$$

$$Z_{\text{off}}^A = 1 + \frac{a}{K_1^A}, \quad (29)$$

$$Z_{\text{on}}^B = q + w_{01}^B q \frac{a}{K_1^B} + w_{02}^B q \frac{b}{K_2^B} + (w_{01}^B + w_{02}^B) w_{12}^B q \frac{a}{K_1^B} \frac{b}{K_2^B} \quad (\text{additive}), \quad (30)$$

$$Z_{\text{on}}^B = q + w_{01}^B q \frac{a}{K_1^B} + w_{02}^B q \frac{b}{K_2^B} + w_{01}^B w_{02}^B w_{12}^B q \frac{a}{K_1^B} \frac{b}{K_2^B} \quad (\text{multiplicative}), \quad (31)$$

$$Z_{\text{off}}^B = 1 + \frac{a}{K_1^B} + \frac{b}{K_2^B} + w_{12}^B \frac{a}{K_1^B} \frac{b}{K_2^B}, \quad (32)$$

$$Z_{\text{on}}^G = q + w_{02}^G q \frac{b}{K_2^G}, \quad (33)$$

$$Z_{\text{off}}^G = 1 + \frac{b}{K_2^G}. \quad (34)$$

Topology D is shown in Fig. 6D; its partition functions are

$$Z_{\text{on}}^A = q + w_{01}^A q \frac{a}{K_1^A} + w_{02}^A q \frac{b}{K_2^A} + (w_{01}^A + w_{02}^A) w_{12}^A q \frac{a}{K_1^A} \frac{b}{K_2^A} \quad (\text{additive}), \quad (35)$$

$$Z_{\text{on}}^A = q + w_{01}^A q \frac{a}{K_1^A} + w_{02}^A q \frac{b}{K_2^A} + w_{01}^A w_{02}^A w_{12}^A q \frac{a}{K_1^A} \frac{b}{K_2^A} \quad (\text{multiplicative}), \quad (36)$$

$$Z_{\text{off}}^A = 1 + \frac{a}{K_1^A} + \frac{b}{K_2^A} + w_{12}^A \frac{a}{K_1^A} \frac{b}{K_2^A}, \quad (37)$$

$$Z_{\text{on}}^B = q + w_{01}^B q \frac{a}{K_1^B}, \quad (38)$$

$$Z_{\text{off}}^B = 1 + \frac{a}{K_1^B}, \quad (39)$$

$$Z_{\text{on}}^G = q + w_{02}^G q \frac{b}{K_2^G}, \quad (40)$$

$$Z_{\text{off}}^G = 1 + \frac{b}{K_2^G}. \quad (41)$$

Topology E is shown in Fig. 6E; its partition functions

are

$$Z_{\text{on}}^A = q + w_{02}^A q \frac{b}{K_2^A}, \quad (42)$$

$$Z_{\text{off}}^A = 1 + \frac{b}{K_2^A}, \quad (43)$$

$$Z_{\text{on}}^B = q + w_{01}^B q \frac{a}{K_1^B} + w_{02}^B q \frac{b}{K_2^B} + (w_{01}^B + w_{02}^B) w_{12}^B q \frac{a}{K_1^B} \frac{b}{K_2^B} \quad (\text{additive}), \quad (44)$$

$$Z_{\text{on}}^B = q + w_{01}^B q \frac{a}{K_1^B} + w_{02}^B q \frac{b}{K_2^B} + w_{01}^B w_{02}^B w_{12}^B q \frac{a}{K_1^B} \frac{b}{K_2^B} \quad (\text{multiplicative}), \quad (45)$$

$$Z_{\text{off}}^B = 1 + \frac{a}{K_1^B} + \frac{b}{K_2^B} + w_{12}^B \frac{a}{K_1^B} \frac{b}{K_2^B}, \quad (46)$$

$$Z_{\text{on}}^G = q + w_{02}^G q \frac{b}{K_2^G}, \quad (47)$$

$$Z_{\text{off}}^G = 1 + \frac{b}{K_2^G}. \quad (48)$$

Topology F is shown in Fig. 6F; its partition functions are

$$Z_{\text{on}}^A = q + w_{01}^A q \frac{a}{K_1^A} + w_{02}^A q \frac{b}{K_2^A} + (w_{01}^A + w_{02}^A) w_{12}^A q \frac{a}{K_1^A} \frac{b}{K_2^A} \quad (\text{additive}), \quad (49)$$

$$Z_{\text{on}}^A = q + w_{01}^A q \frac{a}{K_1^A} + w_{02}^A q \frac{b}{K_2^A} + w_{01}^A w_{02}^A w_{12}^A q \frac{a}{K_1^A} \frac{b}{K_2^A} \quad (\text{multiplicative}), \quad (50)$$

$$Z_{\text{off}}^A = 1 + \frac{a}{K_1^A} + \frac{b}{K_2^A} + w_{12}^A \frac{a}{K_1^A} \frac{b}{K_2^A}, \quad (51)$$

$$Z_{\text{on}}^B = q + w_{01}^B q \frac{a}{K_1^B} + w_{02}^B q \frac{b}{K_2^B} + (w_{01}^B + w_{02}^B) w_{12}^B q \frac{a}{K_1^B} \frac{b}{K_2^B} \quad (\text{additive}), \quad (52)$$

$$Z_{\text{on}}^B = q + w_{01}^B q \frac{a}{K_1^B} + w_{02}^B q \frac{b}{K_2^B} + w_{01}^B w_{02}^B w_{12}^B q \frac{a}{K_1^B} \frac{b}{K_2^B} \quad (\text{multiplicative}), \quad (53)$$

$$Z_{\text{off}}^B = 1 + \frac{a}{K_1^B} + \frac{b}{K_2^B} + w_{12}^B \frac{a}{K_1^B} \frac{b}{K_2^B}, \quad (54)$$

$$Z_{\text{on}}^G = q + w_{02}^G q \frac{b}{K_2^G}, \quad (55)$$

$$Z_{\text{off}}^G = 1 + \frac{b}{K_2^G}. \quad (56)$$

## 2. Stochastic description: Linear noise approximation

The linear noise approximation (LNA) is a second-order expansion of the master equation made under the approximations that (i) mean protein numbers are large and (ii) fluctuations are small compared to means. Under the LNA, the steady state solution to the master equation is a Gaussian distribution: the first-order terms recover the deterministic system and thus provide the means, and the second-order terms yield an equation for the covariance matrix. Comprehensive discussions of the linear noise approximation can be found in [20, 30, 31].

Under the LNA the steady state distribution over each species' protein number is a Gaussian expansion around the deterministic mean given by the steady state of Eqns. 6-8. The covariance matrix  $\Xi$  is determined from model parameters by solving the Lyapunov equation

$$J\Xi + \Xi J^T + D = 0, \quad (57)$$

where  $J$  is the Jacobian of the system (Eqn. 9) and

$$D = \begin{pmatrix} R_A(\alpha + A) & 0 & 0 \\ 0 & R_B(\beta + B) & 0 \\ 0 & 0 & R_G(\gamma + G) \end{pmatrix} \quad (58)$$

is an effective diffusion matrix. We solve Eqn. 57 numerically using MATLAB's `lyap` function.

The deterministic steady state and the covariance matrix are computed four times (once in each of the chemical input states  $c$ ); the lower-right terms of each provide the mean and variance, respectively, of each (Gaussian) output distribution  $p(G|c)$ . The input-output mutual information is computed directly from the distributions  $p(G|c)$ , as described next.

## C. Information theory

In this study we make use of a central measure from information theory: *mutual information* (MI). MI is a fundamental measure of the strength a relationship between two random variables. More precisely, it measures the reduction in entropy of one variable given measurement of the other. MI captures correlation between two random variables even when a relationship exists that is nonlinear (unlike, e.g., the correlation coefficient) or non-monotonic (unlike, e.g., Spearman's rho). It has found wide use in the study of biological networks both as a statistical measure [35, 36] and as a measure of functionality in the presence of noise [16–18]. For a comprehensive review of information theory we refer the reader to [37].

In this study we employ MI in two separate contexts: (i) as a measure of network functionality and (ii) as a measure of statistical correlation. In the first context, we optimize the MI between the chemical input state and the concentration of the output protein. In the second context, we compute, for a given topological feature (e.g.

number of up-regulations), the MI between the value that the feature takes in a network and the function that the network performs. We here describe these computations in turn.

MI is the average of the log of a ratio. The average is over the joint probability distribution between two random variables, and the ratio is that of the joint to the product of the marginal distributions. For a discrete variable, i.e. the chemical input state  $c$ , and a continuous variable, i.e. the output protein concentration  $G$ , MI takes the form

$$I[p(c, G)] = \sum_c \int dG p(c, G) \log_2 \frac{p(c, G)}{p(c)p(G)}, \quad (59)$$

where the log is taken in base 2 to give  $I$  in bits. Noting that  $p(c, G) = p(G|c)p(c)$  and  $p(G) = \sum_c p(c, G)$  allows one to write the MI as

$$I[p(c, G)] = \sum_c \int dG p(G|c)p(c) \log_2 \frac{p(G|c)}{\sum_{c'} p(G|c')p(c')}, \quad (60)$$

i.e. entirely in terms of the conditional output distributions  $p(G|c)$ , obtained via the linear noise approximation (see above), and the input distribution  $p(c)$ , which we take as  $p(c) = 1/4$  for equally likely chemical input states. Eqn. 60 is integrated numerically during the optimization using MATLAB's `quad`.

In the context of correlating, for a topological feature  $\mu$ , the feature value  $v_\mu$  with the observed function  $r$ , since both are categorical (and therefore discrete) variables, MI takes the form

$$I[p(v_\mu, r)] = \sum_{v_\mu, r} p(v_\mu, r) \log \frac{p(v_\mu, r)}{p(v_\mu)p(r)}. \quad (61)$$

Here, the joint distribution  $p(v_\mu, r)$  is computed from the optimization data according to Eqn. 2, and the marginal distributions are trivially obtained as  $p(v_\mu) = \sum_r p(v_\mu, r)$  and  $p(r) = \sum_{v_\mu} p(v_\mu, r)$ .

Additionally we note that MI is again used in the context of statistical correlation to compute a feature adjacency matrix (see Sec. V F). That is, the MI between the values of a feature  $\mu$  and a feature  $\nu$  is given by

$$I[p(v_\mu, v_\nu)] = \sum_{v_\mu, v_\nu} p(v_\mu, v_\nu) \log \frac{p(v_\mu, v_\nu)}{p(v_\mu)p(v_\nu)}, \quad (62)$$

where  $p(v_\mu, v_\nu)$  is computed directly from the network set.

#### D. Optimization

Optimization of input-output information  $I[p(G, c)]$  (Eqn. 60) over model parameters is done numerically using MATLAB's `fminsearch`. Each optimization is performed at constrained average protein number  $N \equiv$

Parameter	Bounds
Promoter strengths, $s$	$10^{-4} - 10^6$
Interaction strengths, $w > 1$ (up-regulation)	$1.05 - 10^2$
Interaction strengths, $w < 1$ (down-regulation)	$10^{-2} - 0.95$
Binding constants, $K$	$10^{-1} - 10^2$
Leakiness, $q$	$10^{-10} - 10^{-2}$
Scaling factors, $x > 1, y > 1$	$1.1 - 10^4$
Degradation rates, $R_A, R_B$	$10^{-7} - 10^0$
Degradation rate, $R_G$ (fixed)	$4 \cdot 10^{-4}$

TABLE II: Bounds from which parameters are drawn to initialize optimization.

$(A + B + G)/3$  and average timescale separation  $T \equiv [(R_A + R_B)/2]/R_G$  by maximizing the quantity

$$L \equiv I[p(G, c)] - \eta N - \kappa T \quad (63)$$

for various values of the Lagrange multipliers  $\eta$  and  $\kappa$  ( $R_G$  is fixed). The optimization is initialized by sampling uniform-randomly in the logs of the parameters; bounds from which initial parameters are drawn are given in Table II.

#### E. Robustness of $\rho$ ranking

The correlation between topological feature value  $v_\mu$  and network function  $r$  is measured for each feature  $\mu$  using a normalized mutual information  $\rho_\mu$ . This measure is a function of the joint distribution  $p(v_\mu, r)$ , whose computation (Eqn. 2) depends on two distributions which we take to be uniform: (i)  $p(n)$ , the probability of observing each network  $n$ , and (ii)  $p(\vartheta|n)$ , the probability of observing each optimally functional point  $\vartheta$  in the parameter space of network  $n$ . Here we show that the ranking of the  $\rho_\mu$  is robust to perturbations in the uniformity of each of these distributions.

##### 1. Perturbing $p(n)$

The uniformity of  $p(n)$  is perturbed by artificially setting  $p(n) \propto (u_n)^\epsilon$ , where  $u_n$  is a vector of random numbers and  $\epsilon$  tunes the entropy of the distribution  $H[p(n)]$ . That is,  $\epsilon = 0$  recovers the maximum-entropy (uniform) distribution, while  $\epsilon \rightarrow \infty$  produces the zero-entropy solution  $p(n) \rightarrow \delta(n, \arg\max u_n)$  (where  $\delta$  is the Kronecker delta). Fig. 7A plots the  $\rho_\mu$  as a function of the entropy  $H[p(n)]$ . As seen in Fig. 7A, the ranking of the top 4 features is preserved under  $\sim 15\%$  perturbations in the entropy, and that of the top 3 features is preserved under  $\sim 30\%$  perturbations. This demonstrates that the feature ranking is considerably robust to perturbations in the uniformity of  $p(n)$ .

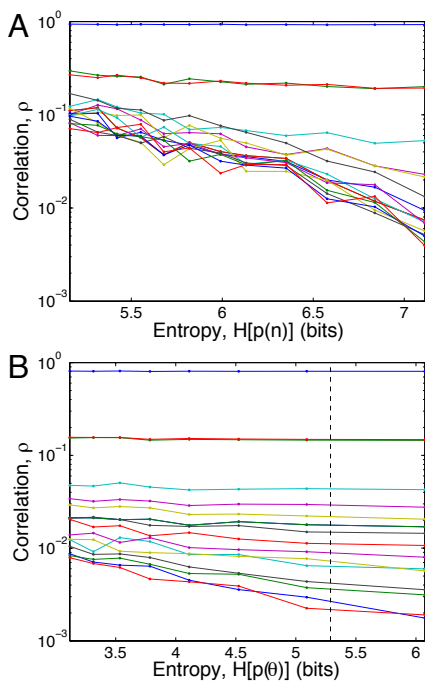


FIG. 7: Values of the correlation measure  $\rho$  for each of the 17 features as a function of the entropies (A)  $H[p(n)]$  and (B)  $H[p(\vartheta|n)]$ . Each point represents the average of 8 trials. In B, the dashed vertical line shows the entropy under the assumption that  $p(\vartheta_0|n)$ , not  $p(\vartheta|n)$ , is uniform.

## 2. Perturbing $p(\vartheta|n)$

The uniformity of  $p(\vartheta|n)$  for each network  $n$  is perturbed via the same procedure described in the previous section. Fig. 7B plots the  $\rho_\mu$  as a function of the entropy of  $p(\vartheta) = \sum_n p(\vartheta|n)p(n)$ , where  $p(n)$  here is uniform. As seen in Fig. 7B, the ranking of the top 7 features is preserved under  $\sim 40\%$  perturbations in the entropy of  $p(\vartheta)$ , indicating that the feature ranking is very robust to perturbations in  $p(\vartheta|n)$ .

In this case we also have an independent entropy scale, given by the fact that we may decompose  $p(\vartheta|n)$  as

$$p(\vartheta|n) = \sum_{\vartheta_0} p(\vartheta|\vartheta_0, n)p(\vartheta_0|n), \quad (64)$$

where  $\vartheta_0$  is the parameter setting that initializes an optimization and  $p(\vartheta|\vartheta_0, n)$  is determined by the optimization itself. If we assume uniformity of  $p(\vartheta_0|n)$ , instead of  $p(\vartheta|n)$ , then  $p(\vartheta|n)$  is computable from the numbers of times the optimization converges repeatedly on each local optimum  $\vartheta$ . The entropy in this case is 13% different from that of the uniform distribution, and the ranking of  $\rho$  is almost entirely unchanged (Fig. 7B). Fig. 7B demonstrates that the results are not sensitive to whether one takes the distribution of initial parameters or the distribution of optimal parameters to be uniform.

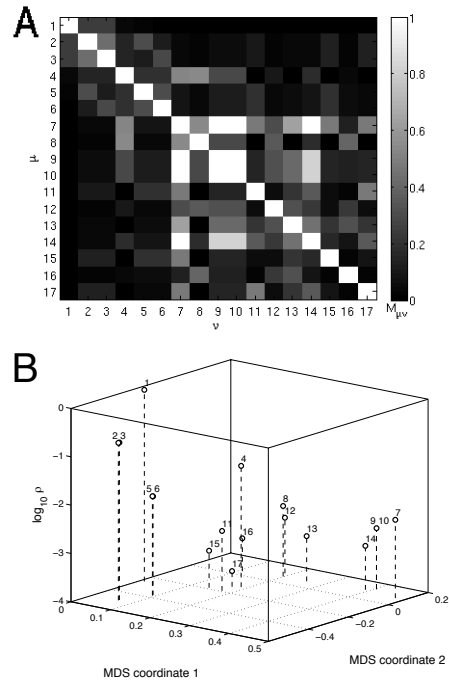


FIG. 8: Identifying non-redundant topological features. (A) Feature adjacency matrix (Eqn. 65). (B) Features plotted according to correlation measure  $\rho$  and the coordinates of a two-dimensional scaling based on the adjacency matrix in A. Features are numbered as in Table I.

## F. Non-redundant features

To interpret which features are associated with which sets of realizable functions, it is useful to group nearly identical features together and use only the feature which is most informative about function (highest in  $\rho$ ) as the exemplar among each group. To quantify redundancy among features, we compute the MI between each pair of features and normalize by the minimum entropy to produce a weighted adjacency matrix

$$M_{\mu\nu} = \frac{I[p(v_\mu), v_\nu]}{\min\{H[p(v_\mu)], H[p(v_\nu)]\}} \quad (65)$$

(Fig. 8A). We then use the adjacency matrix as the basis for multidimensional scaling, as described below.

Multidimensional scaling (MDS) describes a class of techniques used to visualize proximities among data in a low-dimensional space. One of the most common techniques (also called principal components analysis when applied to a correlation matrix) is to use as the low-dimensional coordinates the eigenvectors of the adjacency matrix corresponding to the largest-magnitude eigenvalues. Data points with high mutual proximity then tend to be grouped together along these coordinates. Fig. 8B and Fig. 5 show the application of this technique in two and one dimensions, respectively, to the adjacency matrix in Fig. 8A, revealing groups of similar

features. Plotting the feature-function correlation measure  $\rho$  along the vertical axis in each case makes apparent the most informative feature in each group (i.e. feature 1 in one group and feature 4 in a second group).

### G. Direct functionality: validation of known analytic result

In previous work [14] we show analytically that networks in which each species is regulated by at most one other species perform only “direct” functions, in which the sign of the effect of an input species on an output species depends only on the direct path from input to output, even when there is feedback. This analytic result is here validated by our statistical approach.

In the context of our setup (see Fig. 1A), the direct paths from the inputs (the chemical inhibitors labeled by  $x$  and  $y$ ) to the output (the fluorescent protein  $G$ ) involve only the forward regulatory edges  $A \rightarrow B$  and  $B \rightarrow G$ . Therefore considering only those networks in which each species is singly regulated (Fig. 6A-B), the analytic result predicts that the signs of the forward edges uniquely determine the type of function performed. Plotting the conditional distribution  $p(r|v)$  for the feature ‘signs of the forward edges’ using only data from these networks confirms that this is indeed the case (Fig. 9). Accordingly the correlation for this distribution is  $\rho = 1$ , the maximum possible value.

The functions performed at each of the feature values in Fig. 9 can be understood intuitively. For example, in networks with the last feature value  $A \rightarrow B \rightarrow G$ , inhibition of  $A$  and of  $B$  will both reduce the expression of  $G$ , such that the state in which both small molecules are present ( $++$ ) produces the lowest-ranked output, and conversely, the state in which both small molecules are absent ( $--$ ) produces the highest-ranked output; one may verify by inspection that functions 7 and 8 are the two that satisfy these criteria. The correspondence of the other function pairs to feature values can be similarly understood in terms of the edge signs.

### H. XOR functionality: analysis

As described in the main text, XOR functions satisfy one or both of two properties:

XOR property I:  $\text{sign}(dG/dx)$  depends on  $y$ , (66)

XOR property II:  $\text{sign}(dG/dy)$  depends on  $x$ . (67)

To analytically understand the observed XOR functionality, we here calculate the derivatives  $dG/dx$  and  $dG/dy$  from the steady state of the deterministic system (Eqns. 6-8). We further show how the forms of these derivatives support the observations that (i) all XOR functions satisfying property I are performed by networks in which species  $B$  is autoregulated, and (ii) no functions satisfying property II are observed.

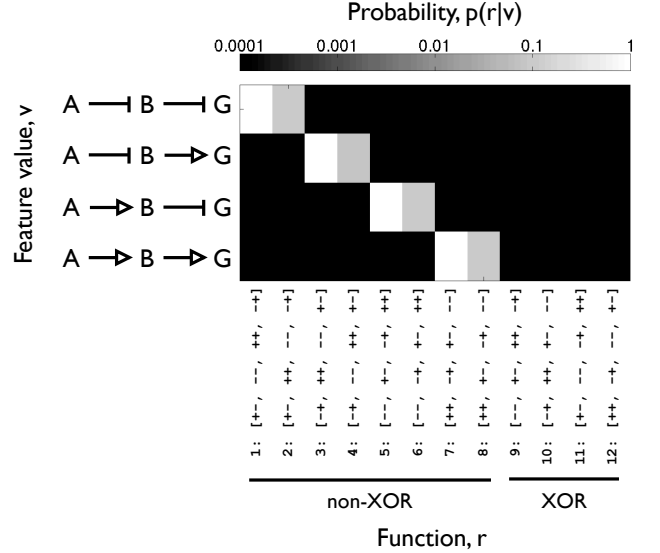


FIG. 9: Conditional distribution showing the probability of a particular input-output function given the value of the topological feature ‘signs (up- or down-regulating) of the forward regulatory edges,’ using only data from networks in which each species is singly regulated (Fig. 6A-B). Only direct functions are performed, as defined in the text.

#### 1. Calculating the derivatives

The steady state of Eqns. 6-8, with all functional dependencies made explicit, is

$$A = \alpha[a(A, x), b(B, y)], \quad (68)$$

$$B = \beta[a(A, x), b(B, y)], \quad (69)$$

$$G = \gamma[b(B, y)], \quad (70)$$

where  $a(A, x) = A/x$  and  $b(B, y) = B/y$ . The output  $G$  depends on the input  $x$  only through  $b$ , and  $b$  depends on  $x$  only through  $B$ , i.e.

$$\frac{dG}{dx} = \frac{d\gamma}{dx} = \frac{d\gamma}{db} \frac{\partial b}{\partial B} \frac{dB}{dx}. \quad (71)$$

The dependencies of  $A$  and  $B$  on  $x$  are coupled:

$$\frac{dA}{dx} = \frac{d\alpha}{dx} = \frac{\partial\alpha}{\partial a} \frac{da}{dx} + \frac{\partial\alpha}{\partial b} \frac{db}{dx} \quad (72)$$

$$= \frac{\partial\alpha}{\partial a} \left( \frac{\partial a}{\partial A} \frac{dA}{dx} + \frac{\partial a}{\partial x} \right) + \frac{\partial\alpha}{\partial b} \left( \frac{\partial b}{\partial B} \frac{dB}{dx} \right), \quad (73)$$

$$\frac{dB}{dx} = \frac{d\beta}{dx} = \frac{\partial\beta}{\partial a} \frac{da}{dx} + \frac{\partial\beta}{\partial b} \frac{db}{dx} \quad (74)$$

$$= \frac{\partial\beta}{\partial a} \left( \frac{\partial a}{\partial A} \frac{dA}{dx} + \frac{\partial a}{\partial x} \right) + \frac{\partial\beta}{\partial b} \left( \frac{\partial b}{\partial B} \frac{dB}{dx} \right). \quad (75)$$

Eqns. 73 and 75 form an algebraic system of equations in the variables  $dA/dx$  and  $dB/dx$ , whose solution is

$$\frac{dA}{dx} = \frac{1}{-\Delta} \left[ \frac{\partial\alpha}{\partial a} \frac{\partial a}{\partial x} \left( 1 - \frac{\partial\beta}{\partial b} \frac{\partial b}{\partial B} \right) + \frac{\partial\alpha}{\partial b} \frac{\partial b}{\partial B} \frac{\partial\beta}{\partial a} \frac{\partial a}{\partial x} \right], \quad (76)$$

$$\frac{dB}{dx} = \frac{1}{-\Delta} \frac{\partial\beta}{\partial a} \frac{\partial a}{\partial x}, \quad (77)$$

where

$$\Delta = \begin{pmatrix} \frac{\partial\alpha}{\partial b} & \frac{\partial b}{\partial B} \\ \frac{\partial\beta}{\partial a} & \frac{\partial a}{\partial A} \end{pmatrix} \begin{pmatrix} \frac{\partial\beta}{\partial a} & \frac{\partial a}{\partial A} \\ -\left( \frac{\partial\alpha}{\partial a} \frac{\partial a}{\partial A} - 1 \right) & \left( \frac{\partial\beta}{\partial b} \frac{\partial b}{\partial B} - 1 \right) \end{pmatrix} \quad (78)$$

$$= \frac{\partial\alpha}{\partial B} \frac{\partial\beta}{\partial A} - \left( \frac{\partial\alpha}{\partial A} - 1 \right) \left( \frac{\partial\beta}{\partial B} - 1 \right) \quad (79)$$

is the determinant of the Jacobian of the dynamical system and is always negative at stable fixed points (Eqn. 11). Substituting Eqn. 77 into Eqn. 71 and using  $\partial\gamma/\partial B = (\partial\gamma/\partial b)(\partial b/\partial B)$  yields Eqn. 4 of the main text,

$$\frac{dG}{dx} = \frac{1}{-\Delta} \frac{\partial a}{\partial x} \frac{\partial\beta}{\partial a} \frac{\partial\gamma}{\partial B}. \quad (80)$$

The output  $G$  depends on the input  $y$  through  $b$ , which depends on  $y$  either indirectly through  $B$  or directly, i.e.

$$\frac{dG}{dy} = \frac{d\gamma}{dy} = \frac{d\gamma}{db} \frac{db}{dy} = \frac{d\gamma}{db} \left( \frac{\partial b}{\partial B} \frac{dB}{dy} + \frac{\partial b}{\partial y} \right). \quad (81)$$

As on  $x$ , the dependencies of  $A$  and  $B$  on  $y$  are coupled:

$$\frac{dA}{dy} = \frac{d\alpha}{dy} = \frac{\partial\alpha}{\partial a} \frac{da}{dy} + \frac{\partial\alpha}{\partial b} \frac{db}{dy} \quad (82)$$

$$= \frac{\partial\alpha}{\partial a} \left( \frac{\partial a}{\partial A} \frac{dA}{dy} \right) + \frac{\partial\alpha}{\partial b} \left( \frac{\partial b}{\partial B} \frac{dB}{dy} + \frac{\partial b}{\partial y} \right), \quad (83)$$

$$\frac{dB}{dy} = \frac{d\beta}{dy} = \frac{\partial\beta}{\partial a} \frac{da}{dy} + \frac{\partial\beta}{\partial b} \frac{db}{dy} \quad (84)$$

$$= \frac{\partial\beta}{\partial a} \left( \frac{\partial a}{\partial A} \frac{dA}{dy} \right) + \frac{\partial\beta}{\partial b} \left( \frac{\partial b}{\partial B} \frac{dB}{dy} + \frac{\partial b}{\partial y} \right). \quad (85)$$

Eqns. 83 and 85 can be solved to yield

$$\frac{dA}{dy} = \frac{1}{-\Delta} \frac{\partial\alpha}{\partial b} \frac{\partial b}{\partial y}, \quad (86)$$

$$\frac{dB}{dy} = \frac{1}{-\Delta} \left[ \frac{\partial\beta}{\partial b} \frac{\partial b}{\partial y} \left( 1 - \frac{\partial\alpha}{\partial a} \frac{\partial a}{\partial A} \right) + \frac{\partial\beta}{\partial a} \frac{\partial a}{\partial A} \frac{\partial\alpha}{\partial b} \frac{\partial b}{\partial y} \right], \quad (87)$$

where  $\Delta$  is the determinant as in Eqn. 79. Substituting Eqn. 87 into Eqn. 81 and simplifying gives Eqn. 5 of the main text,

$$\frac{dG}{dy} = \frac{1}{-\Delta} \left( 1 - \frac{\partial\alpha}{\partial A} \right) \frac{\partial b}{\partial y} \frac{d\gamma}{db}, \quad (88)$$

where  $\partial\alpha/\partial A = (\partial\alpha/\partial a)(\partial a/\partial A)$ .

## 2. Type-I XOR functions require autoregulation of $B$

Type-I XOR functionality (Eqn. 66) requires the sign of the derivative  $dG/dx$  (Eqn. 80) to depend on  $y$ . Here we go through each term in Eqn. 80 and conclude that only the third can change sign. The first term in Eqn. 80,  $1/(-\Delta)$ , is always positive because the determinant  $\Delta$  is equal to the product of the three eigenvalues of the Jacobian of the deterministic system, which at a stable fixed point are all negative (Eqn. 11). The second term in Eqn. 80 is  $\partial a/\partial x = -A/x^2$ , which is always negative, corresponding to the inhibitory effect of the small molecule  $x$  on transcription factor  $A$ . The fourth term in Eqn. 80 is  $\partial\gamma/\partial B = (\partial\gamma/\partial b)(\partial b/\partial B)$ . The factor  $\partial b/\partial B = 1/y$  is always positive, and the factor  $\partial\gamma/\partial b$  is of unique sign because  $\gamma(b)$  is monotonic, as shown below. This leaves only the third term,  $\partial\beta/\partial a$ , which can change sign if and only if  $B$  is autoregulated, as discussed below.

Under our model a regulation function with only one argument is monotonic, which is consistent with the interpretation of the edge being either up- or down-regulating. For example, the regulation function corresponding to the edge  $B \rightarrow G$  in all networks is (see Eqns. 14-15)

$$\gamma(b) = \frac{s_G}{R_G} \frac{Z_{\text{on}}^G}{Z_{\text{on}}^G + Z_{\text{off}}^G}, \quad (89)$$

where  $Z_{\text{on}}^G$  and  $Z_{\text{off}}^G$  are given by, e.g., Eqns. 20-21. The derivative of this function with respect to its argument is

$$\frac{d\gamma}{db} = \frac{s_G}{R_G Z_G^2} \left( \frac{dZ_{\text{on}}^G}{db} Z_{\text{off}}^G - Z_{\text{on}}^G \frac{dZ_{\text{off}}^G}{db} \right), \quad (90)$$

where  $Z_G = Z_{\text{on}}^G + Z_{\text{off}}^G$ . Upon differentiating and inserting Eqns. 20 and 21, all dependence on  $b$  inside the parentheses cancels, leaving

$$\frac{d\gamma}{db} = \frac{s_G q}{R_G K_2^G Z_G^2} (w_{02}^G - 1). \quad (91)$$

Eqn. 91 confirms that  $\gamma(b)$  is monotonic, with  $w_{02}^G > 1$  corresponding to up-regulation, and  $w_{02}^G < 1$  corresponding to down-regulation.

If species  $B$  is not autoregulated, then it is only regulated by species  $A$ ; the regulation function then only has one argument, i.e.  $\beta(a, b) = \beta(a)$ , and, as with  $\gamma(b)$  above, it is monotonic. Therefore without autoregulation of  $B$ , type-I XOR functionality is not possible. We now compute the derivative  $\partial\beta/\partial a$  in the case of two arguments to analytically demonstrate the converse: that with autoregulation of  $B$ , type-I XOR functionality is possible.

As with Eqn. 90, the partial derivative of  $\beta(a, b)$  with respect to  $a$  takes the form

$$\frac{\partial\beta}{\partial a} = \frac{s_B}{R_B Z_B^2} \left( \frac{\partial Z_{\text{on}}^B}{\partial a} Z_{\text{off}}^B - Z_{\text{on}}^B \frac{\partial Z_{\text{off}}^B}{\partial a} \right), \quad (92)$$

where  $Z_B = Z_{\text{on}}^B + Z_{\text{off}}^B$ ,  $Z_{\text{on}}^B$  (with  $B$  autoregulated) is given by, e.g., Eqn. 30 for additive interaction and Eqn. 31 for multiplicative interaction, and  $Z_{\text{off}}^B$  is given by, e.g., Eqn. 32. Upon differentiating and inserting the expressions for  $Z_{\text{on}}^B$  and  $Z_{\text{off}}^B$ , all dependence on  $a$  inside the parentheses cancels (for both additive and multiplicative interaction), leaving

$$\frac{\partial\beta}{\partial a} = \frac{s_B q}{R_B K_1^B Z_B^2} (C_2 b^2 + C_1 b + C_0), \quad (93)$$

where for additive interaction,

$$C_0 = w_{01}^B - 1, \quad (94)$$

$$C_1 = \frac{1}{K_2^B} [w_{01}^B - w_{02}^B - w_{12}^B + (w_{01}^B + w_{02}^B) w_{12}^B], \quad (95)$$

$$C_2 = \left(\frac{1}{K_2^B}\right)^2 w_{01}^B w_{12}^B, \quad (96)$$

and for multiplicative interaction,

$$C_0 = w_{01}^B - 1, \quad (97)$$

$$C_1 = \frac{1}{K_2^B} [w_{01}^B - w_{02}^B - w_{12}^B + w_{01}^B w_{02}^B w_{12}^B], \quad (98)$$

$$C_2 = \left(\frac{1}{K_2^B}\right)^2 (w_{01}^B - 1) w_{02}^B w_{12}^B. \quad (99)$$

Eqn. 93 is the product of a positive term and a quadratic function of  $b = B/y$ . It is straightforward to demonstrate in both the additive and multiplicative cases (e.g. by sampling numerically) that for positive  $w_{01}^B$ ,  $w_{02}^B$ , and  $w_{12}^B$  the quadratic function can have positive, negative, or complex roots. When at least one root is positive, the sign of  $\partial\beta/\partial a$  changes at positive  $B/y$ , i.e. the sign can depend on  $y$ . Since  $dG/dx$  is proportional to  $\partial\beta/\partial a$  (Eqn. 80), this enables type-I XOR functionality. This analysis suggests inspection of the parameters themselves obtained via optimization; doing so, we observe that the vast majority of observed XOR functions results from optimal parameter values for which there exists a positive root in the range  $0 < B/y < \sim 100$ , which is precisely the range of protein numbers in which our optimal solutions lie.

To summarize, nonmonotonicity in the regulation of species  $B$ , which can occur only when  $B$  is autoregulated, produces the observed XOR functions.

### 3. Type-II XOR functions are not observed

Type-II XOR functionality (Eqn. 67) requires the sign of the derivative  $dG/dy$  (Eqn. 88) to depend on  $x$ . Three

of the terms in Eqn. 88 are of unique sign: the terms  $1/(-\Delta)$  and  $d\gamma/db$  are positive and of unique sign respectively, as discussed in the previous section; and the term  $\partial b/\partial y = -B/y^2$  is always negative, corresponding to the inhibitory effect of the small molecule  $y$  on transcription factor  $B$ . This leaves only the term  $(1 - \partial\alpha/\partial A)$ , which, as discussed below, for four of the network topologies is provably positive at stable fixed points, and for the other two network topologies is observed to be positive for all optimal solutions.

For topologies B and E (Fig. 6), in which  $\partial\alpha/\partial A = 0$ , the term  $(1 - \partial\alpha/\partial A) = 1$  is clearly positive. For topologies A and C, in which  $\partial\alpha/\partial B = 0$ , the first eigenvalue of the Jacobian (Eqn. 10) reduces to  $\lambda_1 = \partial\alpha/\partial A - 1$ ; since this must be negative for stability, the term  $(1 - \partial\alpha/\partial A)$  is always positive for these topologies as well. This leaves only networks with topology D or F.

In networks with topology D or F, It is unclear whether type-II XOR functions are analytically forbidden or simply exceedingly improbable for optimally informative parameters. Some analytic constraints can be obtained by the facts that since the real parts of  $\lambda_1$  and  $\lambda_2$  (Eqn. 10) are negative at stable fixed points, their sum must be negative and their product must be positive, i.e.

$$0 < -(\lambda_1 + \lambda_2) = \left(1 - \frac{\partial\alpha}{\partial A}\right) + \left(1 - \frac{\partial\beta}{\partial B}\right), \quad (100)$$

$$0 < \lambda_1 \lambda_2 = \left(1 - \frac{\partial\alpha}{\partial A}\right) \left(1 - \frac{\partial\beta}{\partial B}\right) - \frac{\partial\alpha}{\partial B} \frac{\partial\beta}{\partial A}. \quad (101)$$

If  $(1 - \partial\beta/\partial B) < 0$ , then Eqn. 100 implies that  $(1 - \partial\alpha/\partial A) > 0$ , forbidding type-II XOR functions. If on the other hand  $(1 - \partial\beta/\partial B) > 0$ , Eqn. 100 does not restrict the sign of  $(1 - \partial\alpha/\partial A)$ , but Eqn. 101 implies

$$\left(1 - \frac{\partial\alpha}{\partial A}\right) > \frac{(\partial\alpha/\partial B)(\partial\beta/\partial A)}{1 - \partial\beta/\partial B}. \quad (102)$$

Although in this last case it is not known whether the right-hand side is constrained to be positive, empirically the term  $(1 - \partial\alpha/\partial A) > 0$  is observed to be positive for all optimal solutions, even over wide variations in the orders of magnitude of each of the optimal parameters across solutions.

### Acknowledgments

The authors thank Nicolas Buchler and William Bialek for useful conversations. AM was supported by NSF grant DGE-0742450; CHW was supported by NIH grants 1U54CA121852-01A1 and 5PN2EY016586-03.

[1] Thompson, D (1917) *On Growth and Form* (Cambridge University Press).

[2] Sherrington, SC (1906) *The integrative action of the ner-*



- vous system* (New Haven, CT: Yale University Press).
- [3] Stricker, J et al. (2008) A fast, robust and tunable synthetic gene oscillator. *Nature* 456:516–9.
  - [4] Gardner, TS, Cantor, CR, Collins, JJ (2000) Construction of a genetic toggle switch in *Escherichia coli*. *Nature* 403:339–42.
  - [5] Elowitz, MB, Leibler, S (2000) A synthetic oscillatory network of transcriptional regulators. *Nature* 403:335–8.
  - [6] Cusick, ME, Klitgord, N, Vidal, M, Hill, DE (2005) Interactome: gateway into systems biology. *Hum Mol Genet* 14 Spec No. 2:R171–81.
  - [7] Schena, M, Shalon, D, Davis, RW, Brown, PO (1995) Quantitative monitoring of gene expression patterns with a complementary DNA microarray. *Science* 270:467–70.
  - [8] Giot, L et al. (2003) A protein interaction map of *Drosophila melanogaster*. *Science* 302:1727.
  - [9] Guet, CC, Elowitz, MB, Hsing, W, Leibler, S (2002) Combinatorial synthesis of genetic networks. *Science* 296:1466–70.
  - [10] Basu, S, Mehreja, R, Thiberge, S, Chen, MT, Weiss, R (2004) Spatiotemporal control of gene expression with pulse-generating networks. *Proc Natl Acad Sci USA* 101:6355–60.
  - [11] Mangan, S, Zaslaver, A, Alon, U (2003) The coherent feedforward loop serves as a sign-sensitive delay element in transcription networks. *J Mol Biol* 334:197–204.
  - [12] Strogatz, SH (2000) *Nonlinear dynamics and chaos: With applications to physics, biology, chemistry, and engineering* (Westview Press).
  - [13] Ziv, E, Nemenman, I, Wiggins, CH (2007) Optimal signal processing in small stochastic biochemical networks. *PLoS ONE* 2:e1077.
  - [14] Mugler, A, Ziv, E, Nemenman, I, Wiggins, CH (2008) Serially regulated biological networks fully realise a constrained set of functions. *IET Syst Biol* 2:313–322.
  - [15] Mugler, A, Ziv, E, Nemenman, I, Wiggins, CH (2009) Quantifying evolvability in small biological networks. *IET Syst Biol* 3:379–387.
  - [16] Tkacik, G, Callan, CG, Bialek, W (2008) Information flow and optimization in transcriptional regulation. *Proc Natl Acad Sci USA* 105:12265–70.
  - [17] Mehta, P, Goyal, S, Long, T, Bassler, BL, Wingreen, NS (2009) Information processing and signal integration in bacterial quorum sensing. *Mol Syst Biol* 5:325.
  - [18] Walczak, AM, Tkačik, G, Bialek, W (2010) Optimizing information flow in small genetic networks. II. Feedforward interactions. *Phys. Rev. E* 81:41905.
  - [19] Gillespie, DT (1977) Exact stochastic simulation of coupled chemical reactions. *J Phys Chem* 81:2340–2361.
  - [20] Paulsson, J (2004) Summing up the noise in gene networks. *Nature* 427:415–8.
  - [21] Elowitz, MB, Levine, AJ, Siggia, ED, Swain, PS (2002) Stochastic gene expression in a single cell. *Science* 297:1183–6.
  - [22] Walczak, AM, Mugler, A, Wiggins, CH (2009) A stochastic spectral analysis of transcriptional regulatory cascades. *Proc Natl Acad Sci USA* 106:6529.
  - [23] Mugler, A, Walczak, AM, Wiggins, CH (2009) Spectral solutions to stochastic models of gene expression with bursts and regulation. *Phys. Rev. E* 80:041921.
  - [24] Buchler, NE, Gerland, U, Hwa, T (2003) On schemes of combinatorial transcription logic. *Proc Natl Acad Sci USA* 100:5136–41.
  - [25] Bintu, L et al. (2005) Transcriptional regulation by the numbers: models. *Curr Opin Genet Dev* 15:116–24.
  - [26] Bintu, L et al. (2005) Transcriptional regulation by the numbers: applications. *Curr Opin Genet Dev* 15:125–35.
  - [27] Kaplan, S, Bren, A, Zaslaver, A, Dekel, E, Alon, U (2008) Diverse two-dimensional input functions control bacterial sugar genes. *Mol Cell* 29:786–92.
  - [28] Cox, RS, Surette, MG, Elowitz, MB (2007) Programming gene expression with combinatorial promoters. *Mol Syst Biol* 3:145.
  - [29] Mayo, AE, Setty, Y, Shavit, S, Zaslaver, A, Alon, U (2006) Plasticity of the cis-regulatory input function of a gene. *PLoS Biol* 4:e45.
  - [30] Elf, J, Ehrenberg, M (2003) Fast evaluation of fluctuations in biochemical networks with the linear noise approximation. *Genome Research* 13:2475–84.
  - [31] van Kampen, NG (1992) *Stochastic processes in physics and chemistry* (Amsterdam: North-Holland).
  - [32] Borg, I, Groenen, PJF (2005) *Modern multidimensional scaling: Theory and applications, 2nd ed.* (New York, NY: Springer-Verlag).
  - [33] Hermsen, R, Ursem, B, ten Wolde, PR (2010) Combinatorial gene regulation using auto-regulation. *PLoS Comput Biol* 6:e1000813.
  - [34] Guptasarma, P (1995) Does replication-induced transcription regulate synthesis of the myriad low copy number proteins of *Escherichia coli*? *Bioessays* 17:987–97.
  - [35] Margolin, AA et al. (2006) ARACNE: an algorithm for the reconstruction of gene regulatory networks in a mammalian cellular context. *BMC Bioinformatics* 7:S7.
  - [36] Ziv, E, Middendorf, M, Wiggins, CH (2005) Information-theoretic approach to network modularity. *Physical Review E* 71:046117.
  - [37] Cover, TM, Thomas, JA (1991) *Elements of Information Theory* (John Wiley and Sons, New York, NY).